© 2017. Published by The Company of Biologists Ltd | Journal of Cell Science (2017) 130, 2564-2578 doi:10.1242/jcs.197905

RESEARCH ARTICLE

Importin-β and CRM1 control a RANBP2 spatiotemporal switch essential for mitotic kinetochore function

Eugenia Gilistro[1], Valeria de Turris[2], Michela Damizia[1], Annalisa Verrico[1], Sara Moroni[1], Riccardo De Santis[2,3], Alessandro Rosa[2,3] and Patrizia Lavia[1,*]

ABSTRACT

Protein conjugation with small ubiquitin-related modifier (SUMO) is a post-translational modification that modulates protein interactions and localisation. RANBP2 is a large nucleoporin endowed with SUMO E3 ligase and SUMO-stabilising activity, and is implicated in some cancer types. RANBP2 is part of a larger complex, consisting of SUMO-modified RANGAP1, the GTP-hydrolysis activating factor for the GTPase RAN. During mitosis, the RANBP2–SUMO-RANGAP1 complex localises to the mitotic spindle and to kinetochores after microtubule attachment. Here, we address the mechanisms that regulate this localisation and how they affect kinetochore functions. Using proximity ligation assays, we find that nuclear transport receptors importin-β and CRM1 play essential roles in localising the RANBP2–SUMO-RANGAP1 complex away from, or at kinetochores, respectively. Using newly generated inducible cell lines, we show that overexpression of nuclear transport receptors affects the timing of RANBP2 localisation in opposite ways. Concomitantly, kinetochore functions are also affected, including the accumulation of SUMO-conjugated topoisomerase-IIα and stability of kinetochore fibres. These results delineate a novel mechanism through which nuclear transport receptors govern the functional state of kinetochores by regulating the timely deposition of RANBP2.

KEY WORDS: RANBP2, Importin-β, CRM1/exportin 1, Kinetochore function, Proximity ligation assay

INTRODUCTION

Protein conjugation with SUMO (small ubiquitin-related modifier) peptides is a post-translational modification of growing importance in cell division (reviewed by Wan et al., 2012; Flotho and Werner, 2012; Eifler and Vertegaal, 2015). SUMO addition modifies the interaction surfaces of proteins and can modulate their interaction profile, localisation or function. Indeed, SUMO conjugation often targets and 'rewires', and/or relocates proteins acting in rapid responses and dynamic signalling processes.

RAN-binding protein 2 (RANBP2; also known as NUP358, nucleoporin of 358 kDa), is the largest nucleoporin (NUP) in nuclear pore complexes (NPCs). It is endowed with SUMO E3-type ligase activity (Pichler et al., 2002). Overlapping with the SUMO ligase domain is a binding domain for SUMO-conjugated proteins (SUMO-interacting motif, SIM), which RANBP2 uses to associate with, and stabilise, SUMO-conjugated proteins (Werner et al., 2012). RANBP2 has a modular structure (Wu et al., 1995; Yokoyama et al., 1995) that includes four RAN-GTPase-binding domains (RBDs), phenyl/glycine (FG)-rich regions shared with other NUPs, a zinc-finger region and a cyclophilin-homologous domain.

A major RANBP2 target is RANGAP1, the GTP-hydrolysis activating factor for the GTPase RAN. RANBP2 associates with and stabilises SUMOylated RANGAP1 (SUMO-RANGAP1) through the SIM domain and tethers it to NPCs (Matunis et al., 1996, 1998; Mahajan et al., 1997), while unconjugated RANGAP1 is soluble in the cytoplasm. In turn, RANGAP1 association with RANBP2 reinforces its SUMO E3 activity: RANBP2 and RANGAP1 are actually viewed as components of a multimeric SUMO ligase unit that also includes the E2 SUMO-conjugating enzyme UBC9, known as the RRSU (RANBP2–RANGAP1-SUMO–UBC9) complex (Werner et al., 2012).

RANBP2 and SUMO-RANGAP1 associate throughout the cell cycle (Swaminathan et al., 2004). After nuclear envelope (NE) breakdown and NPC disassembly, they both localise to mitotic microtubules (MTs) and a fraction accumulates at kinetochores (KTs) after MT attachment (Joseph et al., 2002). RANGAP1 localisation to KTs requires SUMOylation and RANBP2 function (Joseph et al., 2004).

In addition to RANBP2–SUMO-RANGAP1, SUMO-specific isopeptidases also reside at centromeres and KTs (Zhang et al., 2008; Cubeñas-Potts et al., 2015) and play roles in centromere and KT functions (Mukhopadhyay and Dasso, 2010; Cubeñas-Potts et al., 2013). These findings suggest that cycles of SUMOylation and deSUMOylation modulate proteins in KT-directed mitotic processes that ultimately govern chromosome segregation (Wan et al., 2012).

Both RANGAP1 and RANBP2 play roles in MT nucleation and stability. RANGAP1 decreases the local RANGTP concentration at KTs. In physiological mitosis, RANGTP activates KT-directed nucleation of MTs (Tulu et al., 2006) that contribute to the spindle organisation (reviewed by Cavazza and Vernos, 2015; Prosser and Pelletier, 2017). KT-associated RANGAP1 is critical to RANGTP turnover at KTs, and hence to modulation of KT-directed MT nucleation and K-fibre stability (Torosantucci et al., 2008). RANBP2 also plays a role in MT nucleation and stabilisation. That role is critical in the presence of specific mutations found in certain cancers (e.g. BRAF mutations). Remarkably, RANBP2 confers a 'vulnerability' to those cancers by rendering them sensitive to the MT-targeting drug vinorelbine (Vecchione et al., 2016).

The RRSU complex also facilitates the disassembly of export complexes (Ritterhoff et al., 2016) formed by the nuclear export vector exportin-1 (CRM1; chromosome region maintenance 1),

[1]CNR National Research Council of Italy, Institute of Molecular Biology and Pathology (IBPM), % Department of Biology and Biotechnology, Sapienza Università di Roma, Via degli Apuli 4, 00185 Rome, Italy. [2]Istituto Italiano di Tecnologia, Center for Life Nanoscience@Sapienza, Viale Regina Elena 291, 00161 Rome, Italy. [3]Department of Biology and Biotechnology 'Charles Darwin', Sapienza University of Rome, Piazzale Aldo Moro 5, 00185 Rome, Italy.

*Author for correspondence (patrizia.lavia@uniroma1.it)

P.L., 0000-0003-3310-6701

Received 26 September 2016; Accepted 5 June 2017

Journal of Cell Science (2017) 130, 2564-2578 doi:10.1242/jcs.197905

cargo proteins carrying nuclear export signals (NES), and RANGTP, which stabilises the complex. In nuclear export, RANGAP1 activates RANGTP hydrolysis at the NPC and initiates export complex disassembly and release of the NES cargo. RRSU complexes at MT-attached KTs (Joseph et al., 2004) may similarly facilitate the release of KT proteins harbouring NES signals. Understanding how the RRSU complex is itself regulated in space and time during mitosis is therefore a relevant question.

Both RANBP2 and RANGAP1 interact with nuclear transport receptors during nuclear transport cycles. RANBP2 interacts via FG-rich domains with importin-β, the main vector of protein import in interphase nuclei. RANBP2 is the most cytoplasmic NUP, and interacts with importin-β in the initial steps of the import cycle, i.e. when import complexes assembled in the cytoplasm dock to the NPC to traverse it (Bednenko et al., 2003; Christie et al., 2016). After NE breakdown, importin-β associates with mitotic MTs (Ciciarello et al., 2004) and interacts with spindle-associated and MT-regulatory factors. The binding to importin-β keeps these factors inactive (Ciciarello et al., 2007; Clarke and Zhang, 2008; Kalab and Heald, 2008), hence keeping mitotic progression on schedule by preventing the premature onset of mitotic events; importin-β acts therefore as a global negative regulator of mitosis (reviewed by Forbes et al., 2015). When overexpressed, importin-β causes an array of mitotic abnormalities (Nachury et al., 2001; Ciciarello et al., 2004; Kaláb et al., 2006), including the inhibition of RANGAP1 localisation to KTs (Roscioli et al., 2012).

RANBP2 and RANGAP1 also interact with CRM1, the export vector for proteins out of the nucleus. The former uses a zinc finger-containing domain (Singh et al., 1999). The latter contains several NES motifs and requires CRM1 for its cytoplasmic localisation (Cha et al., 2015). During mitosis, CRM1 fractions localise at centrosomes (Forgues et al., 2003; Budhu and Wang, 2005), MTs and KTs (Arnaoutov et al., 2005; Zuccolo et al., 2007; Wu et al., 2013). The KT-associated CRM1 fraction is required to localise several proteins therein, including SUMO-RANGAP1 and RANBP2 (Arnaoutov et al., 2005).

These findings implicate nuclear transport receptors in the mitotic localisation of the RRSU complex. The underlying mechanisms, and the functional consequences for mitotic progression, remain unclear, however. If nuclear transport receptors contribute to determine the RRSU complex localisation, they should also determine the sites of RANBP2-dependent SUMOylation of mitotic proteins and influence processes that depend upon it.

To address these questions, we have visualised the interactions between transport factors and the RANBP2–SUMO-RANGAP1 complex during mitosis. Using proximity ligation assays (PLAs) and inducible cell lines to modulate the expression of each transport factor, we find that importin-β and CRM1 have opposite functions in a finely tuned mechanism that regulates the RANBP2-RANGAP1 complex at mitotic MTs and KTs, respectively. Through this mechanism, importin-β and CRM1 influence mitotic processes that require RANBP2 activity, including the KT localisation of SUMO-conjugated topoisomerase II alpha (TOP2A), and the stability of KT microtubules, or K-fibres.

RESULTS

RANBP2 interactions with nuclear transport receptors are spatially and temporally regulated before and after MT attachment to chromosomes

Most RAN network components and effectors are shuttling proteins and establish dynamic interactions that have been difficult to depict in whole cells without resorting to expressing exogenous tagged proteins. The PLA technique visualises interactions between native proteins located in close proximity (within 30 nm) *in situ* (see Materials and Methods). In human mitotic cells, it was used to visualise interacting members of the chromosomal passenger complex (Vuoriluoto et al., 2011).

We took advantage of PLA technology to analyse RRSU interactions in mitotic HeLa cells. In pilot experiments, we selected known interacting pairs, i.e. RANBP2-RANGAP1 and RAN-CRM1. PLA signals for both combinations accumulated at the nuclear rim, and, to a lesser extent in the cytoplasm for RANBP2-RANGAP1 and in the nucleus for RAN-CRM1 (Fig. S1), as expected from the localisation of single proteins. No signal was observed in PLA reactions using antibodies to RANBP2 and a non-expressed protein, i.e. GFP (data not shown).

We then investigated PLA products formed by RANBP2 and nuclear transport receptors. In interphase, RANBP2 PLA products with both importin-β (Fig. 1A) and CRM1 (Fig. 1C) were restricted to the NE region, visualised by lamin B1, consistent with the resident nature of RANBP2 at NPCs.

To follow the redistribution of RANBP2–importin-β PLA products from interphase to mitosis, we stained cells for lamin B1, MTs (α-tubulin) and KTs (CREST antibody) (Fig. S2A). This showed a progressive relocalisation of RANBP2–importin-β PLA signals from the interphase NE rim to MTs: as the NE deforms under centrosomal pushing, and eventually breaks down, PLA products are released in the cytoplasm and gradually associate with the growing mitotic MTs. In prometaphase, abundant PLA signals accumulate at MTs. Most signals can be inscribed within the profiles of the forming half spindles and excluded from chromosomes (Fig. 1B, top row). As MT-KT attachments are established and chromosomes become bioriented, PLA signals decrease. In anaphase, fewer PLA signals are visualised, mostly associated with interpolar rather than KT-bound MTs (stage-specific panels are shown in Fig. S2A).

We next examined the RANBP2-CRM1 combination. Low-abundance PLA products were detected at MTs in early mitosis, which increased in metaphase. At that stage, PLA signals began to concentrate at the outer CREST-stained KTs and remained associated with KTs during segregation in anaphase (detailed mitotic progression in Fig. S2B). In telophase, when the spindle disassembled, PLA products for both the RANBP2–importin-β and RANBP2-CRM1 combinations relocalised around chromatin, indicating that the NE was reforming. The PLA patterns are consistent with the immunofluorescence (IF) localisation of individual components (Joseph et al., 2002, 2004; Ciciarello et al., 2004; Arnaoutov et al., 2005; Wu et al., 2013). Thus, the PLA approach visualises interacting, or closely associated, endogenous RANBP2 and nuclear transport receptors, and can depict variations in these interactions at the intracellular site at which they occur.

Although PLA cannot measure the absolute amount of interacting proteins within cells, as it entails an amplification step, the PLA patterns suggested that RANBP2 interactions varied before and after MT attachment to chromosomes. We compared quantitative estimates of PLA signals either manually or automatically (counting every single PLA signal as an object; details in Materials and Methods), with consistent results; henceforth the automatic mode was used unless specified otherwise. We counted PLA signals either throughout the cells, or at MTs, or in the chromosome-KT area, then grouped the cells in discrete classes according to their PLA signal content, and compared the profile of prometaphases and metaphases in unperturbed cell populations. In

Journal of Cell Science (2017) 130, 2564-2578 doi:10.1242/jcs.197905

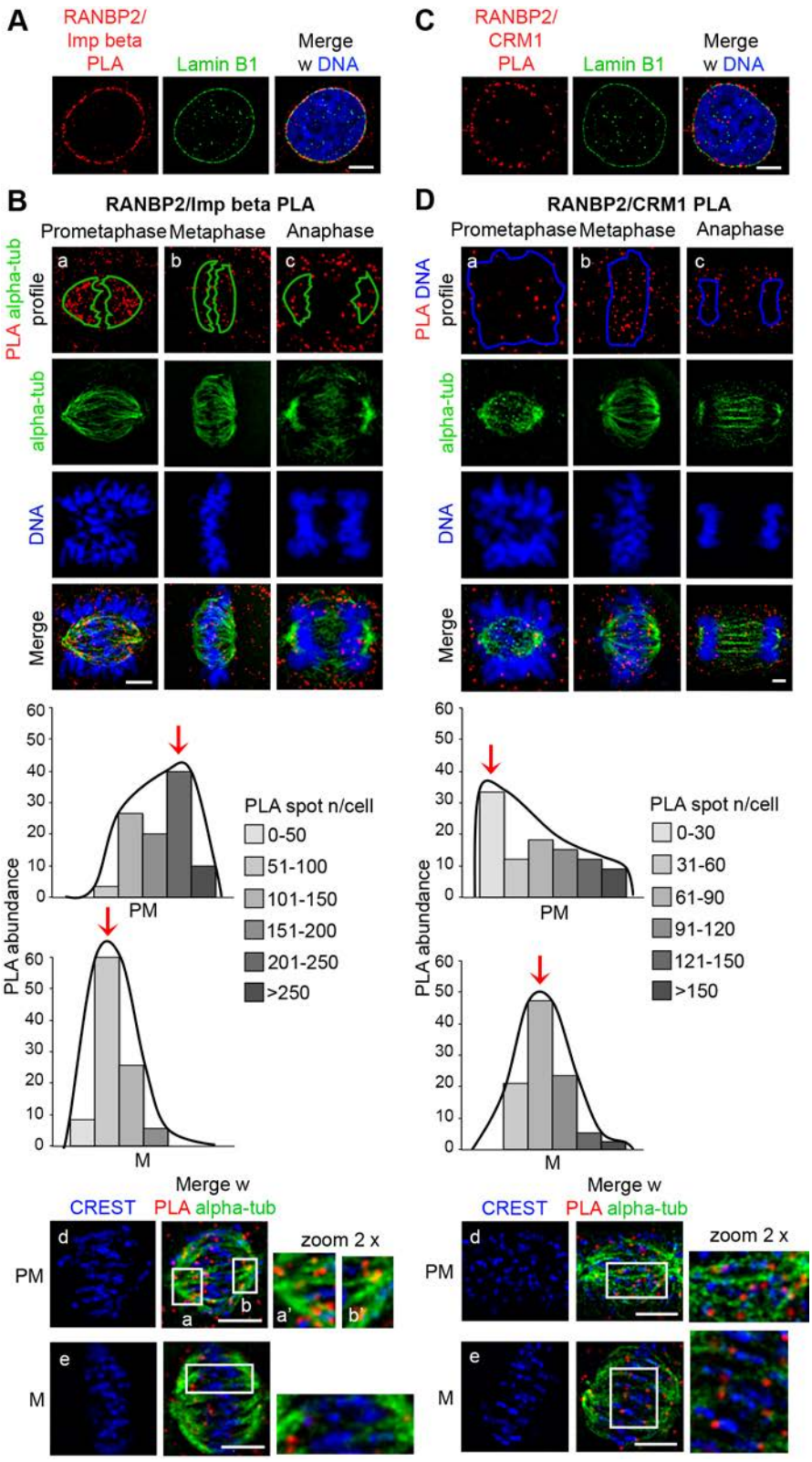

Fig. 1. RANBP2-CRM1 and RANBP2–importin-β PLA products are spatially and temporally regulated in mitosis. (A) In interphase, RANBP2 PLA reactions with importin (Imp)-β are visible at the NE (lamin staining). (B) RANBP2–importin-β PLA signals during mitotic progression. PLA products localise mainly to MTs (delimited by the green profile; MT and chromosome staining are shown below). The graph quantifies RANBP2–importin-β PLA products associated with MTs in mitotic stages: prometaphase (upper panel) and metaphase (lower panel) cells are grouped in discrete classes according to their content of MT-associated PLA products (inset key); the histograms represent the frequency of cells in each class. Red arrows indicate modal classes. The decrease in metaphase versus prometaphase cells was highly significant (P<0.0001, χ^2 test); n=180 prometaphases and 320 metaphases (nine experiments). The IF panels at the bottom show the detail of RANBP2–importin-β PLA products along MTs in prometaphase and metaphase (insets, 2× zoom). (C) Interphase RANBP2-CRM1 PLA products at the NE (lamin staining). (D) RANBP2-CRM1 PLA signals localise at MTs and, after metaphase, in part also at chromosomes (delimited by the blue profile). The histograms represent the frequency of prometaphase versus metaphase cells grouped in classes of abundance of RANBP2-CRM1 PLA products counted in the chromosome KT area. The IF panels at the bottom show that RANBP2-CRM1 PLA products become KT-associated in metaphase (insets, 2× zoom), with a highly significant increase compared with prometaphase (P<0.0005, χ^2 test); n=140 prometaphases and 540 metaphases, nine experiments. Counting the overall number of PLA products in whole cells revealed the same trend and level of statistical significance shown in graphs B and D. Scale bars: 5 µm. Extended images for both pairs during mitotic progression are shown in Fig. S2.

RANBP2–importin-β PLA reactions, we counted significantly fewer signals in metaphases compared with prometaphases, both at spindle MTs (Fig. 1B) and in whole cells (data not shown); thus, metaphase marked a real quantitative decrease of RANBP2 interaction with importin-β, rather than delocalisation from MTs. RANBP2 PLA products with CRM1 showed the opposite trend, with a significant increase from prometaphase to metaphase in whole cells, which coincided with the appearance of PLA products in the chromosome KT region in metaphase (Fig. 1D). In addition, we observed a clear shift in the modal class of abundance of RANBP2-containing PLA products with each one of nuclear transport receptors before and after metaphase alignment.

Journal of Cell Science (2017) 130, 2564-2578 doi:10.1242/jcs.197905

These results suggest that RANBP2 takes part in two distinct associations that include importin-β and CRM1, respectively. These variations suggest that a RANBP2 fraction 'switches partners' from prometaphase, when it forms abundant interactions with importin-β along the spindle MTs, to metaphase, when its association with MTs decreases and PLA signals with CRM1 increase at the level of MT-attached KTs.

To control the PLA specificity, we silenced RANBP2, which should prevent the formation of PLA products. RANBP2-specific siRNAs effectively downregulated RANBP2 abundance compared with controls treated with control siRNAs (GL2, targeting the luciferase gene) (Fig. S3A). As a read-out, SUMOylated RANGAP1 decreased in RANBP2-silenced cells compared with controls (Fig. S3A), which coincided with the absence of RANGAP1 from metaphase KTs in IF images (Fig. S3B). RANBP2-depleted cultures showed lengthened mitotic duration, paralleled by the appearance of multipolar spindles and misaligned chromosomes (Fig. S3C), as expected (Salina et al., 2003; Joseph et al., 2004; Hashizume et al., 2013). In RANBP2-silenced cultures we found no, or very few, PLA signals, for both importin-β–RANBP2 (Fig. S3D) and CRM1-RANBP2 (Fig. S3E) at MTs, KTs and in whole cells. Although importin-β abundance was reported to decrease in RANBP2-interfered cells in other experiments (Hashizume et al., 2013), neither importin-β nor CRM1 abundance displayed significant variations under the conditions used in this study (Fig. S3A); thus downregulation of PLA products truly reflects the loss of RANBP2 protein in silenced cultures, indicating that the PLA technique depicts genuine RANBP2 interactions in mitotic cells.

RANBP2 and RANGAP1 are engaged as a unit in regulated interactions with nuclear transport receptors

Given that SUMO-RANGAP1 associates with RANBP2 throughout the cell cycle (Swaminathan et al., 2004), the localisation of PLA products between RANBP2 and each nuclear transport receptor should parallel that of RANGAP1, or at least a fraction thereof. To test this, we repeated the PLA reactions with nuclear transport receptors using RANGAP1. As with RANBP2, RANGAP1 also formed abundant PLA products with importin-β at the MT level in prometaphase, which decreased in metaphase (Fig. S4A). This suggests that a RANGAP1 fraction associates, directly or via RANBP2, with importin-β in early mitosis and detaches from it when MTs attach to KTs.

Conversely, RANGAP1-CRM1 PLA products increased from prometaphase to metaphase, at which stage they became visible in the chromosome area (Fig. S4B). Interestingly, RANGAP1-CRM1 PLA products were barely detectable when using a CRM1 antibody targeting the CRM1 N-terminal region, which contains the RANGTP-binding domain; the N-terminal CRM1 antibody also failed to detect CRM1 at KTs (Fig. S4C). These observations suggest that CRM1 requires a free RAN-binding domain in order to localise at KTs and recruit RANGAP1 therein; once anchored, the domain is probably not available to the antibody. Direct examination of RANBP2-RANGAP1 PLA products finally revealed signals along MTs in prometaphase, with a fraction accumulating at KTs in metaphase (Fig. S4D).

In summary, both RANBP2 and RANGAP1 establish parallel interactions with importin-β at MTs, which decrease at metaphase, and with CRM1 at MTs and at metaphase KTs. This suggests that they engage as a unit in complementary interactions with nuclear transport receptors with mitotic stage-specific patterns. The partner switch becomes evident after chromosome alignment rather than in prometaphase, when MT-KT interactions are first established. We conclude, therefore, that the event of biorientation, rather than MT-KT contact *per se*, marks a key step in the 'switch partners' model for the RANBP2-RANGAP1 complex.

CRM1 post-transcriptional silencing or functional inhibition downregulate RANBP2-containing PLA products at kinetochores

To assess whether the KT-associated CRM1 fraction plays an active role in the RANBP2 metaphase switch, we inactivated CRM1 in different ways to see how that would affect PLA patterns during mitotic progression. We first silenced CRM1 post-transcriptionally using siRNAs (Fig. 2A). That yielded multipolar mitoses and significant chromosome misalignment and mis-segregation (Fig. 2B), as expected (Arnaoutov et al., 2005). Under these conditions, RANBP2-CRM1 PLA products were severely downregulated, and a substantial proportion of cells displayed no, or rare, PLA signals both in the chromosome KT region (Fig. 2C) and throughout the cell. Thus, although RNA interference protocols may not completely deplete the targeted proteins, and the PLA technique includes an amplification step that can amplify products generated by the residual protein, the CRM1-silencing experiments (Fig. 2A-C) indicate that the stage-specific variations previously depicted using the PLA approach were genuine.

Because the RNA interference protocol took 48–72 h to achieve effective CRM1 silencing, we sought to rule out possible indirect effects caused by long-term alterations in interphase nuclear export. We therefore repeated the PLA assays after short-term treatment with leptomycin B (LMB) to inhibit CRM1 function. CRM1 inhibition was demonstrated by the nuclear retention of RANBP1, a characterised NES-containing export cargo, in interphase (Fig. 2D), and induction of mitotic abnormalities similar to those observed after CRM1 silencing (Fig. 2E). We found that a 2 h pulse of LMB was sufficient to inhibit the formation of CRM1-RANBP2 PLA products in mitotic cells (Fig. 2F). Interestingly, LMB did not affect the formation of RANBP2-RANGAP1 PLA products, but prevented their accumulation at KTs (Fig. S4E). Thus LMB blocks the 'switch partners' step occurring in normal mitotic cells and prevents the localisation of RANBP2-CRM1 PLA products to metaphase KTs.

In summary, loss-of-function experiments validate the 'switch partners' model depicted in PLA assays: they substantiate the conclusion that both RANBP2 and RANGAP1 interact with nuclear transport receptors during mitosis, and highlight a specific shift coinciding with chromosome biorientation: at this time, their interaction with importin-β decreases along the spindle MTs and the complexes with CRM1 increase and accumulate at KTs.

Induction of importin-β overexpression alters RANBP2 interactions and localisation in mitotic cells

At this point we asked whether unbalancing transport factors would perturb the RRSU complex mitotic localisation. Previous studies examined the consequences of importin-β overexpression in mitosis in transient assays, consistently reporting multipolar spindles and chromosome mis-segregation (Nachury et al., 2001; Ciciarello et al., 2004; Kaláb et al., 2006), as well as inhibition of SUMO-RANGAP1 accumulation at KTs (Roscioli et al., 2012). If RRSU moves as a complex, then importin-β overexpression should also influence the localisation of RANBP2 and impact on mitotic processes that depend upon it. To verify this we needed to eliminate the variability associated with transient expression. We established a HeLa cell line with stably integrated EGFP-tagged importin-β under the control of a doxycycline (dox)-inducible promoter (see Materials

Journal of Cell Science (2017) 130, 2564-2578 doi:10.1242/jcs.197905

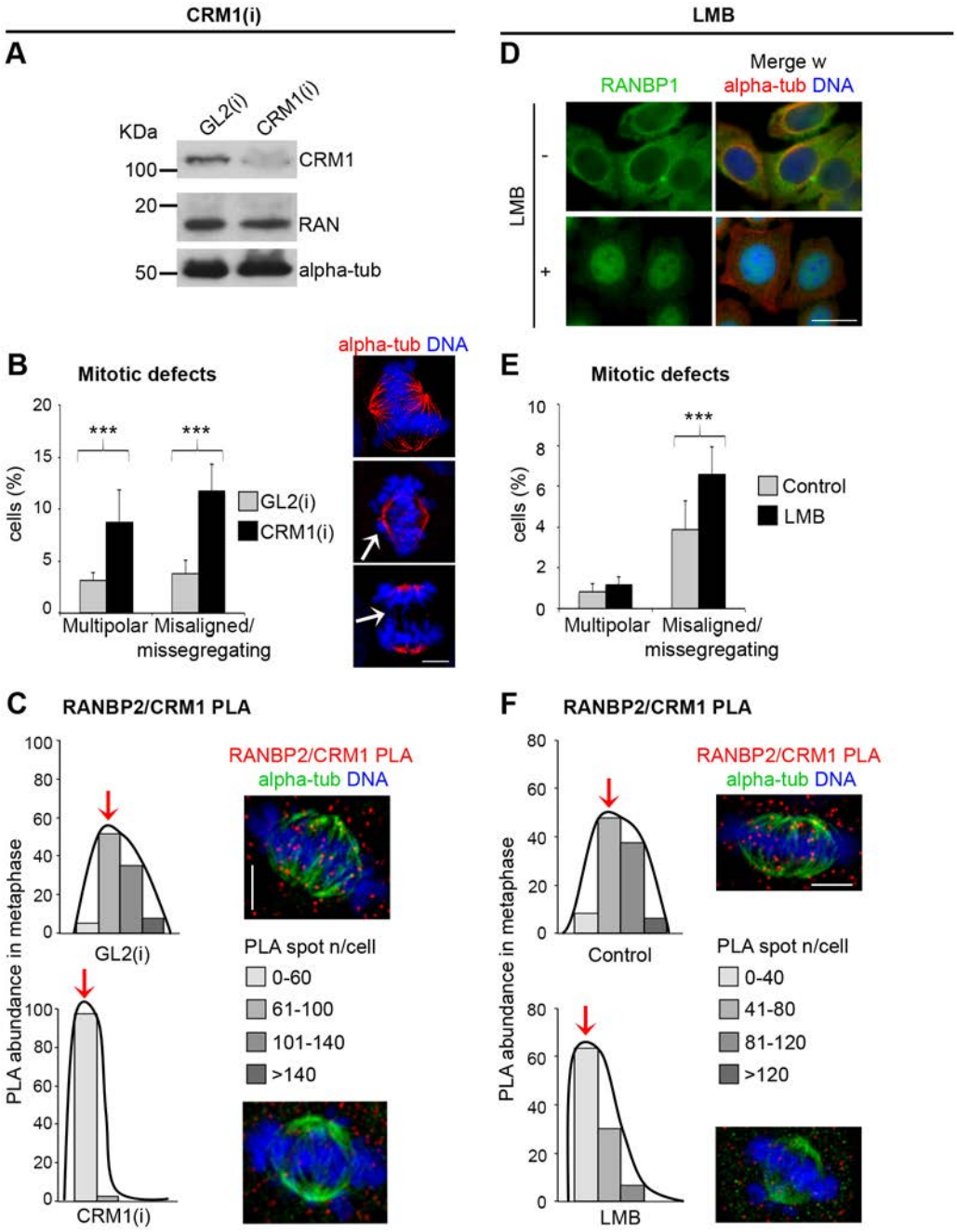

Fig. 2. CRM1 silencing or functional inhibition abolish RANBP2-containing PLA products. (A) CRM1 silencing substantially reduces CRM1 protein levels. (B) Induction of mitotic abnormalities in CRM1-silenced cultures compared with GL2-interfered controls (***P<0.0001, χ^2 test); n≥3000 mitotic cells, three experiments. The IF panels exemplify frequent defects: multipolar spindles (top), misaligned (middle) and mis-segregating chromosomes (bottom). (C) Histograms represent the frequency of mitotic cells grouped in classes of abundance of KT-associated RANBP2-CRM1 PLA products in CRM1-silenced and control (GL2) cells (P<0.025, χ^2 test in two experiments, n=50 cells per condition). (D) LMB abolishes nuclear export of RANBP1 in interphase. (E) Induction of mitotic abnormalities in LMB-treated cultures compared with controls (***P<0.0001, χ^2 test); n≥3400 cells, two experiments. (F) Distribution of mitotic cells in classes of abundance of RANBP2-CRM1 PLA products at KTs, in LMB-treated and control cultures (P<0.0001, χ^2 test); n=60 cells per condition, two experiments. Red arrows indicate modal classes. Scale bars: 5 µm (except in panel D, where scale bar denotes 20 µm).

and Methods). In time-lapse microscopy, all cells expressed importin-β–EGFP with similar intensity starting 3–4 h after dox addition. Overall, importin-β abundance increased by about 1.8-fold 6 h after dox induction, and 2.5-fold after 24 h (Fig. 3A), and overexpressed importin-β–EGFP reproduced the localisation of the endogenous protein at the spindle MTs (Fig. 3B). In time-lapse analysis, mitotic cells underwent lengthened prometaphase and metaphase duration early after importin-β induction (6 h), associated with severe alterations in the spindle bipolarity and/or function; over time (24 h), a significant proportion died during mitosis or in the next interphase (Fig. 3C). Consistent with this, fixed IF-stained cultures showed significant chromosome misalignment and mis-segregation (Fig. 3D). Thus, importin-β overexpression, albeit mild, hinders spindle organisation and function.

We next examined RANBP2 interactions with transport receptors in the importin-β-inducible cell line. We found significantly

Journal of Cell Science (2017) 130, 2564-2578 doi:10.1242/jcs.197905

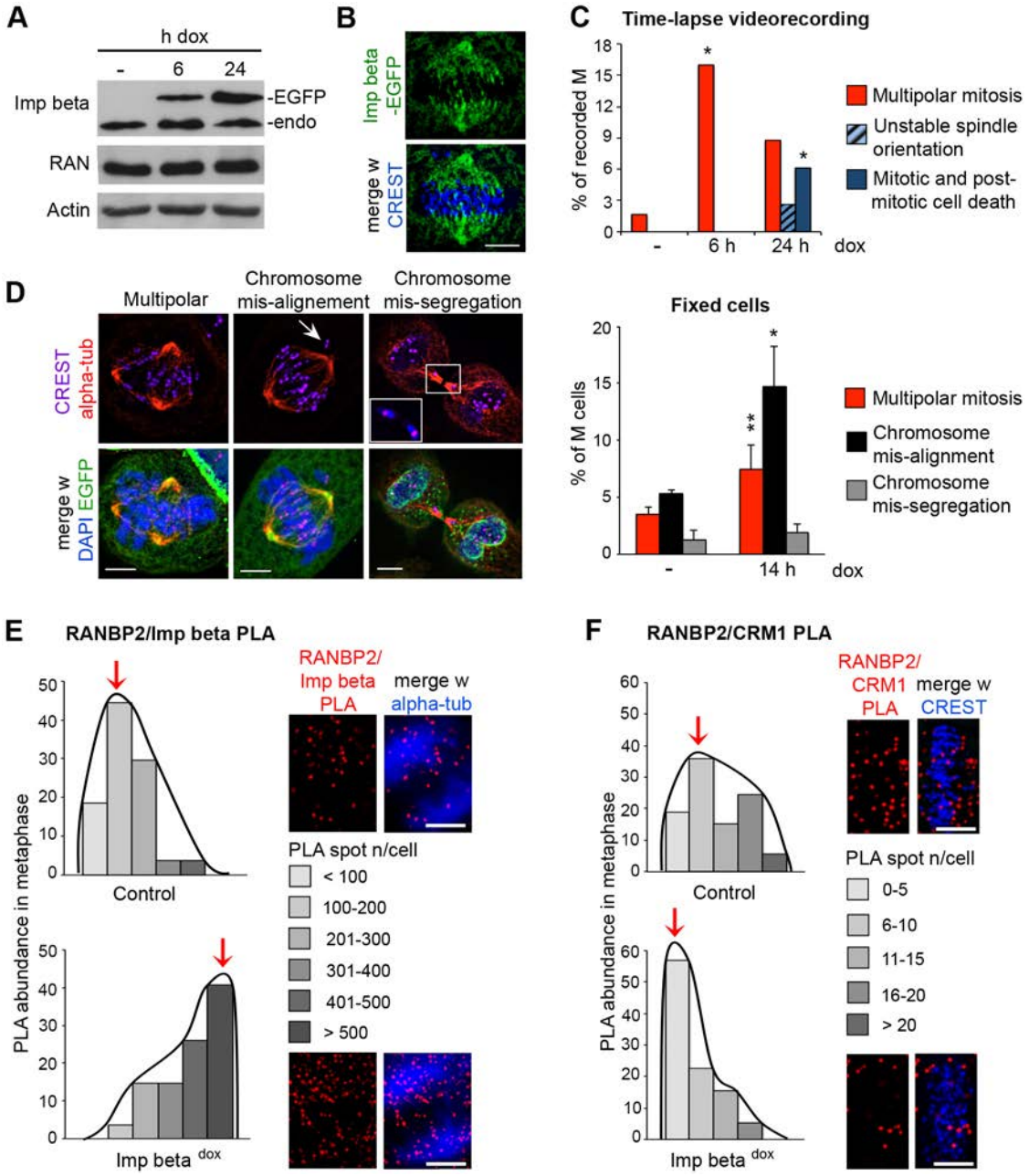

Fig. 3. Importin-β retains RANBP2 at MTs and decreases its association with CRM1. (A) Cell extracts were probed with importin-β antibody after dox induction. The upper importin-β band corresponds to dox-induced EGFP chimaera, the lower band is the endogenous protein. (B) Dox-induced importin-β-EGFP reproduces the endogenous protein localisation at spindle MTs. (C) Time-lapse imaging data, showing the evolution of mitotic abnormalities recorded 6 or 24 h after importin-β induction (*P<0.01 compared with controls, χ^2 test); n≥115 mitoses per time point, three experiments. (D) The IF panels exemplify mitotic abnormalities in fixed dox-induced cell samples (multipolar mitosis, misaligned metaphase chromosome, lagging chromosome in telophase), quantified in the histograms (*P<0.01, **P<0.0005 compared with controls, χ^2 test); n≥500 mitotic cells, two experiments. (E) Histograms represent the distribution of metaphases according to their abundance of importin-β–RANBP2 PLA signals in the MT area (blue spindles), showing a highly significant increase in importin-β-induced compared with control cells (P<0.0001, χ^2 test); n≥128 cells per condition, three experiments. (F) Histograms represent the distribution of metaphases according to their content of CRM1-RANBP2 PLA signals localising at KTs (blue), showing a highly significant decrease in importin-β-induced compared with control metaphases (P<0.005, χ^2 test); n=215 metaphases per condition, four experiments. Examples are shown in the IF panels. Scale bars, 5 µm.

increased RANBP2–importin-β PLA signals compared with controls. These signals mostly localised at the spindle MTs and, importantly, remained abundant in metaphase (Fig. 3E), when they normally decrease in non-induced cells. Concomitantly, RANBP2-CRM1 PLA products were downregulated in whole cells, and hardly any signal was seen at metaphase chromosomes, in induced compared with non-induced cultures (Fig. 3F). Thus, increased importin-β levels retain RANBP2 at MTs, and prevent the shift in the balance between MT-bound and KT-bound RRSU complex that takes place in metaphase.

CRM1 overexpression alters the timing of RANBP2-dependent interactions in mitosis

We asked whether inducing elevated CRM1 levels would symmetrically affect RANBP2 mitotic interactions. We generated a dox-inducible CRM1-EGFP HeLa cell line using the same vector

Journal of Cell Science (2017) 130, 2564-2578 doi:10.1242/jcs.197905

as for importin-β (see Materials and Methods). CRM1-EGFP expression was detected by time-lapse microscopy about 3–4 h after dox administration in stable cell lines. Dox induction yielded a mild but reproducible increase in CRM1 expression (about 1.4-fold after 6 h, and 2-fold after 24 h) (Fig. 4A), and overexpressed CRM1 reproduced the localisation of the endogenous protein at the spindle, with a fraction at KTs in metaphase (Fig. 4B).

Time-lapse recording of CRM1-induced cells showed significant prometaphase and metaphase delay, with a statistically significant fraction of recorded mitoses developing micronucleated and multinucleated phenotypes after 24 h of recording (Fig. 4C). Consistent with the micro-/multi-nucleation phenotypes recorded in live cells, IF analysis of fixed cells depicted misaligned chromosomes in metaphase, as well as abnormal anaphase and

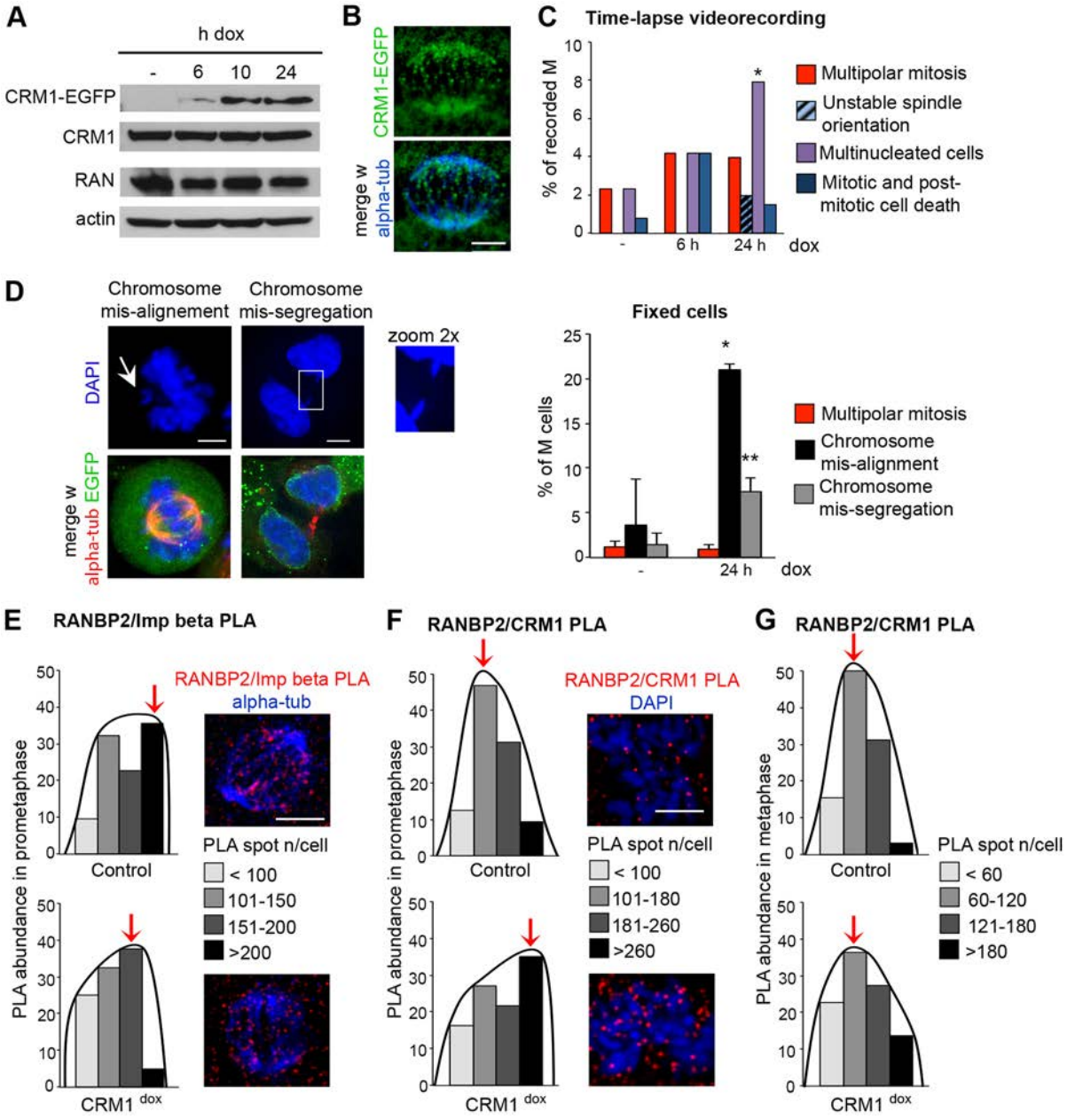

Fig. 4. CRM1 induction anticipates RANBP2 recruitment to KTs and decreases it at MTs. (A) CRM1-EGFP induction by dox. (B) Dox-induced CRM1-EGFP reproduces the endogenous CRM1 localisation. (C) CRM1 induces mitotic abnormalities in time-lapse assays; the histograms represent the frequency of phenotypes recorded 6 or 24 h after CRM1 induction (*P<0.05, χ^2 test); n=130 cells per sample, two experiments. (D) Mitotic abnormalities in fixed IF-stained CRM1-induced cultures: left, metaphase misaligned chromosome; right, failed chromosome segregation in telophase (2× zoom). Abnormalities (quantified in the histograms) increase significantly in CRM1-induced versus control cultures (*P<0.025 and **P<0.001, χ^2 test); n=300 mitotic cells, two experiments. (E) Importin-β–RANBP2 PLA products at MTs (exemplified in the IF panels) in CRM1-induced and control cultures; histograms represent the distribution of metaphases in classes of PLA abundance, and indicate a significant decrease after CRM1 induction (P<0.01, χ^2 test); n=40 metaphases per condition, three experiments. (F) RANBP2-CRM1 PLA signals at KTs significantly increase in CRM1-induced versus non-induced prometaphases. Histograms represent the distribution of prometaphases according to their content of RANBP2-CRM1 PLA products at KTs (P<0.05, χ^2 test); n=40 prometaphases per condition, two experiments. (G) Distribution of metaphase cells according to their content of RANBP2-CRM1 PLA products at KTs: no significant variation (χ^2 test) was observed (45 analysed metaphases per condition, two experiments). Scale bars: 5 µm.

Journal of Cell Science (2017) 130, 2564-2578 doi:10.1242/jcs.197905

telophase figures with chromosomes that failed to segregate (Fig. 4D).

We found that mitotic RANBP2–importin-β PLA products were significantly reduced in CRM1-induced cultures (Fig. 4E), while in parallel cultures, RANBP2-CRM1 products increased in prometaphase compared with non-induced controls (Fig. 4F). In physiological mitoses, RANBP2-CRM1 PLA products reach greatest abundance in metaphase and CRM1 induction did not increase their abundance any further (Fig. 4G). Thus, increased abundance of CRM1 impaired the formation of RANBP2–importin-β PLA products and caused a premature RANBP2 recruitment to prometaphase KTs. Concomitant with this, cells develop severe segregation abnormalities that remain mostly uncorrected, thus originating micronucleated cells.

MTs are essential to RANBP2-RANGAP1 localisation in mitotic cells

Previous assays showed that RANBP2 co-immunoprecipitated with importin-β, with or without MTs (Roscioli et al., 2012), suggesting that MTs are dispensable for their interaction to occur, at least in mitotic cell extracts. To assess whether MTs played any role in supporting RANBP2 interactions in intact cells, we pre-synchronised cells by thymidine arrest and release, and when they reached the G2-M transition, we applied NOC to prevent mitotic MT assembly. Controls were pre-synchronised and left untreated after the block release.

We compared RANBP2–importin-β PLA patterns in NOC-arrested and untreated prometaphases. As a standard we analysed BubR1, a spindle checkpoint component that remains associated with unattached KTs. The results show sparse importin-β–RANBP2 PLA signals throughout mitotic-arrested cells in the NOC samples. The overall abundance of PLA signals, however, did not change in NOC-treated versus untreated cultures (Fig. 5A, left panel), indicating that MTs were not essential for importin-β–RANBP2 PLA product formation.

RANBP2-CRM1 PLA products also showed disperse patterns. We found that manual counting of PLA spots relative to the KTs in single planes was more accurate than automated counting in cells devoid of MTs with widespread chromosomes. After manual counting, the amount of RANBP2-CRM1 PLA signals was again comparable in NOC-treated versus untreated cells (Fig. 5A, right panel). However, different from BubR1 signals that associated with CREST-stained KTs in all planes (Fig. 5B, left), only some of the CRM1-RANBP2 PLA signals genuinely localised at KTs, while a large fraction laid in different planes from KTs (Fig. 5B, right). Thus, NOC decreased the association of CRM1-RANBP2 PLA signals with KTs (Fig. 5C), but did not modify their abundance. In summary, MTs are not required as an assembly platform for RANBP2 PLA product formation with nuclear transport receptors, but they are necessary for their localisation.

Overexpression of CRM1 or importin-β affects SUMOylation of topoisomerase-IIα in opposite ways

The results thus far delineate a dynamic scenario in which the mitotic localisation of RANBP2 depends on the antagonistic activities of importin-β, which retains it at the spindle MTs, versus CRM1, which drives its transfer to KTs after MT attachment. To understand whether this RANBP2 switch might affect KT function, we decided to assess potential RANBP2 SUMOylation substrates after induction of either importin-β or CRM1.

TOP2A plays an important role in decatenation of chromatids to enable segregation. TOP2A localises to chromosomes in early mitosis: in Fig. 6A, TOP2A (leftmost panel) is distributed along the entire chromosome length in prometaphase (upper row) and gradually concentrates at KTs in metaphase (Fig. 6A, lower row) to act in decatenation of sister centromeres. Cells in which this is prevented form chromatin bridges that cannot be resolved in anaphase. These defects can give rise to aneuploid cells (reviewed by Chen et al., 2015). In physiological mitosis, a fraction of TOP2A is SUMOylated (Azuma et al., 2003), and impaired SUMOylation affects the centromere decatenation function of TOP2A (Dawlaty et al., 2008). Both PIAS-gamma (Ryu et al., 2010) and RANBP2 (Dawlaty et al., 2008) are implicated in TOP2A SUMO conjugation: indeed, TOP2A fails to accumulate at inner centromeres in animal models that express lowered RANBP2 levels (Dawlaty et al., 2008).

We wondered whether SUMO conjugation of TOP2A, besides being affected by RANBP2 abundance, is also affected by RANBP2 localisation. To investigate this, we adapted the PLA protocol to detect intramolecular reactions between TOP2A and SUMO-2/3 peptides: this protocol enabled us to visualise SUMO-TOP2A PLA products (representative prometaphase and metaphase PLA patterns are shown in Fig. 6B). By measuring the fraction of SUMO-TOP2A PLA localised at KTs (visualised by CREST) over the entire pool of SUMO-TOP2A PLA throughout the cell (plotted in the graph), it was evident that SUMOylated TOP2A concentrates at KTs in metaphase.

It was interesting at this point to establish whether disrupting the importin-β- and CRM1-dependent system of RANBP2 localisation affected the spatial pattern of SUMO-TOP2A. We first examined CRM1-overexpressing cultures. Because CRM1 overexpression anticipates the formation of RANBP2-CRM1 complexes at prometaphase KTs (see Fig. 4), we focused our analysis on scoring SUMO-TOP2A intramolecular PLA signals in prometaphase figures that showed clearly identifiable isolated KTs, hence MT unattached. We found that CRM1-induced cultures displayed significant SUMO-TOP2A accumulation at MT-unattached KTs compared with non-induced controls (Fig. 6C). We then examined the importin-β-induced cell line, in which the accumulation of RANBP2-CRM1 products at metaphase KTs is impaired (see Fig. 3F). We found that the presence of SUMO-TOP2A signals was also significantly reduced at metaphase KTs in this cell line (Fig. 6D). In summary, therefore, conditions that prevent the RANBP2 ‘switch partners’ model yield a correspondingly altered timing of SUMO-TOP2A localisation at KTs during mitotic progression.

CRM1 and importin-β overexpression affect K-fibre stability

Several studies have implicated both importin-β and CRM1 in MT dynamic activity and stability (reviewed by Dasso, 2006; Ciciarello et al., 2007; Kalab and Heald, 2008; Forbes et al., 2015). Based on the data obtained thus far, we wondered whether these effects attributed to nuclear transport factors might involve RANBP2. To address that question, we decided to analyse cold-induced MT depolymerisation, which is used as an informative assay to measure MT stability. After 20 min on ice, most control metaphases displayed partially polymerised MTs and K-fibres forming disorganised spindles (Fig. 7A, left panel). In the importin-β-induced cell line, most mitotic cells showed only short residual MT fragments (Fig. 7Bb); MT destabilisation was associated with a lack of RANBP2 localisation at KTs (Fig. 7Ba,d). We next analysed MTs in the CRM1 cell line. After 20 min of cold incubation, most mitotic cells retained partially polymerised MTs, with or without CRM1 induction. When the incubation was

Journal of Cell Science (2017) 130, 2564-2578 doi:10.1242/jcs.197905

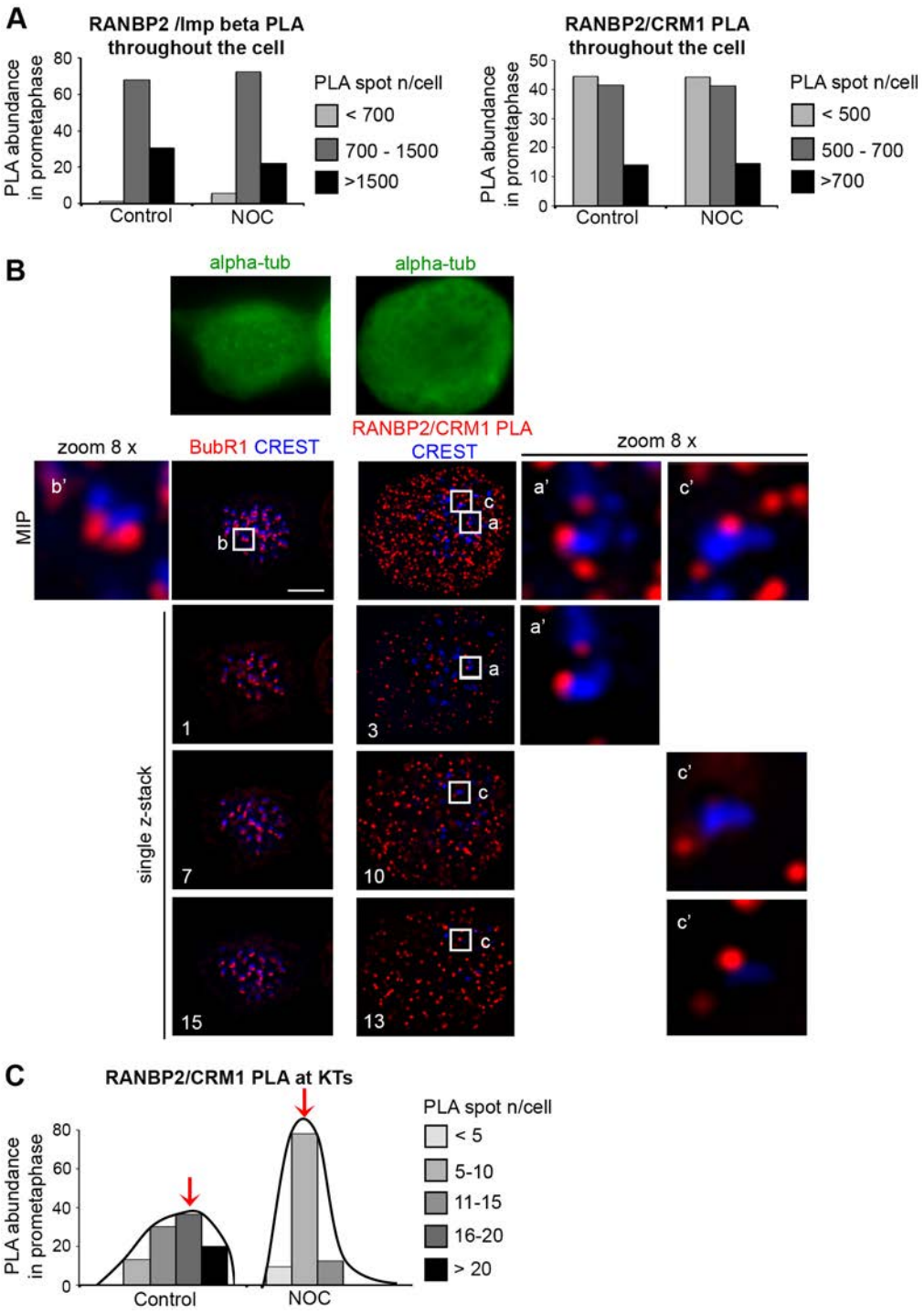

Fig. 5. NOC disrupts the localisation but not the formation of RANBP2-containing PLA products. (A) Intracellular abundance of RANBP2–importin-β (left) and RANBP2-CRM1 (right) PLA products in NOC-arrested and control prometaphases: no statistical difference was observed for either interaction in whole cells, with or without MTs. (B) Co-localisation analysis of RANBP2-CRM1 PLA products and KTs in single planes in NOC-treated cultures. α-tubulin (green) is diffuse, indicating that NOC treatment was effective. Individual planes are shown below the MIP fields. BubR1 signals (left column) co-localise with CREST-stained KTs in all planes (1, 7 and 15 are shown as examples). In the right-hand column, the MIP field shows RANBP2-CRM1 PLA products (red) spread throughout the cell outside KTs (CREST). In single planes of the apparent PLA-CREST associations seen in the MIP image, only some are genuine (stack 3 shows an example of genuine localisation on the outer KT, framed in the MIP field as in a, enlarged in a′); other PLA signals, although apparently overlapping with CREST, in fact do not associate with KTs in individual planes, as the framed example in c in the MIP field: the c' zoom shows the KT at stack 10, whereas the PLA spot lies at stack 13. This dissociation was not seen in cells with unperturbed MTs. a′, b′ and c′, 8× enlargements of a, b and c. Scale bar: 5 µm. (C) The histograms show a dramatic decrease of prometaphases with localised RANBP2-CRM1 PLA products at KTs in NOC-treated cultures (P<0.0001, χ^2 test); n=65 cells, two experiments.

prolonged to 35 min to induce extensive MT depolymerisation, most non-induced cells lacked resistant K-fibres and displayed short MT fragments or tubulin spots over a diffuse background (Fig. 7D, left column). CRM1 induction resulted in more extensive protection from cold depolymerisation and persistence of K-fibres (Fig. 7Eb), associated with RANBP2 accumulation to KTs (Fig. 7Ed).

In summary, importin-β and CRM1 affect the sensitivity of K-fibres to cold-induced depolymerisation in opposite ways, and their ultimate effect over K-fibre stability correlates with their ability to induce the presence or absence of RANBP2 from KTs.

DISCUSSION

RAN GTPase network members, nuclear transport receptors and components of the NPC – through which transport is operated – are now well known to play regulatory roles in mitosis when nucleocytoplasmic transport ceases. They regulate MT nucleation, dynamics and interactions with KTs, largely via physical association with mitotic structures (centrosomes, spindle poles, MTs and KTs), and ultimately contribute to orchestrating chromosome segregation.

Here, we focus on RANBP2, a NUP with well-established mitotic roles (Salina et al., 2003; Joseph et al., 2004; Hashizume et al.,

Journal of Cell Science (2017) 130, 2564-2578 doi:10.1242/jcs.197905

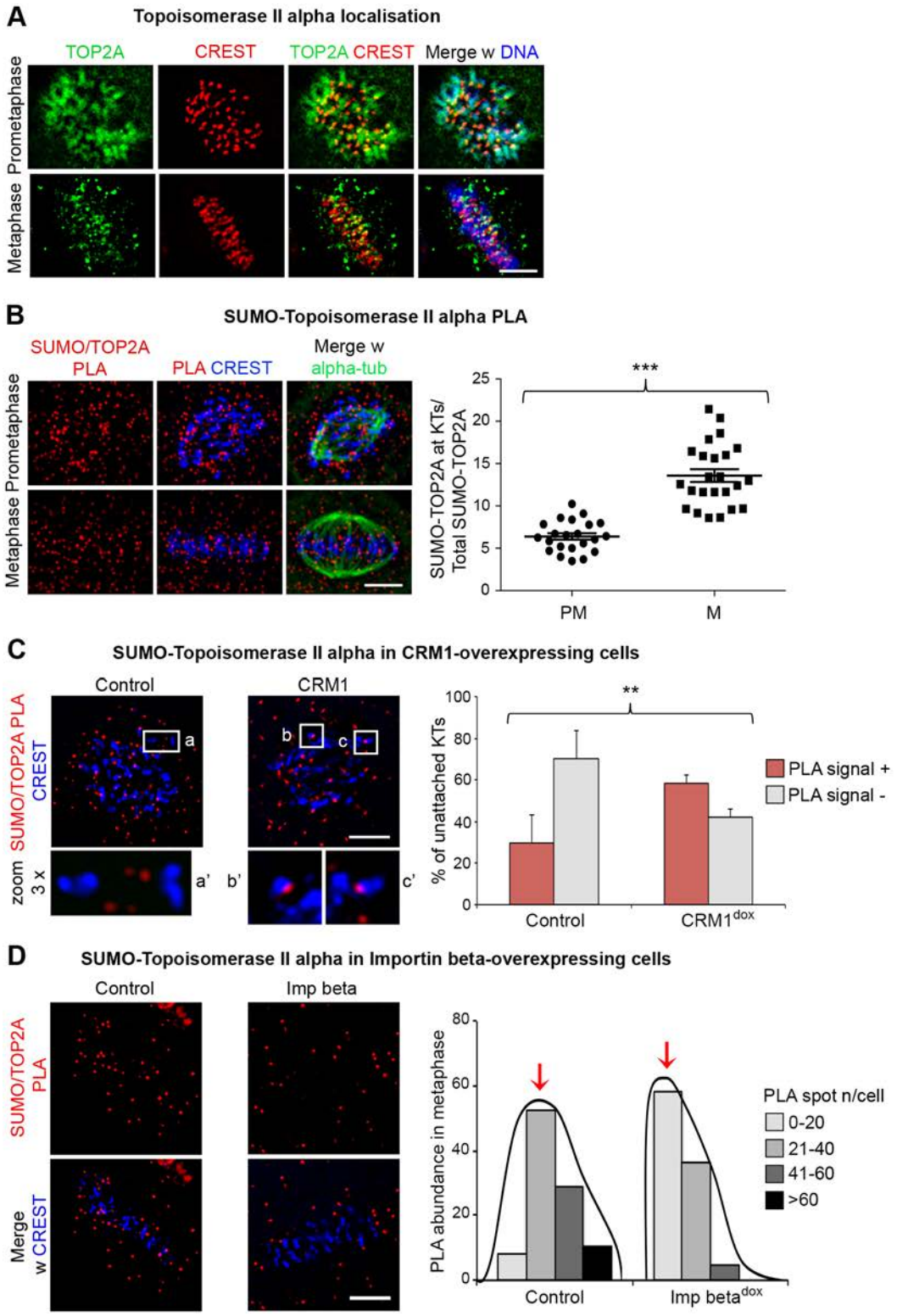

Fig. 6. CRM1 and importin-β affect SUMO-TOP2A accumulation at KTs. (A) In physiological mitosis, TOP2A co-localises with chromosomes in prometaphase (upper row) and concentrates at CREST-stained KTs in metaphase (lower row). (B) Examples of SUMO-TOP2A intramolecular PLA patterns in prometaphase (upper) and metaphase (lower) cells, showing that SUMOylated TOP2A concentrates at KTs in metaphase. In the scatter plot, each point shows the ratio of KT-associated to total SUMO-TOP2A measured in single cells; $P<0.0001$, unpaired *t*-test ($n=22$ prometaphases and 24 metaphases, two independent experiments). (C) In CRM1-overexpressing cells, SUMO-TOP2A localises at unattached KTs in prometaphase (insets, 3× zoom). Histograms represent the frequency of individual unattached KTs that accumulate (red) or are devoid (grey) of SUMO-TOP2A PLA signals, with a significant increase in CRM1-overexpressing cells (**$P<0.005$, χ^2 test); PLA signals were scored at 90 unattached KTs per sample, two experiments. (D) Decreased accumulation of SUMO-TOP2A at metaphase KTs in importin-β-induced cells. The graphs show the distribution of metaphase cells in classes of abundance of SUMO-TOP2A PLA products at KTs: importin-β-overexpressing cultures display a significant decrease compared with controls ($P<0.0001$, χ^2 test); $n=40$ scored metaphases per condition, two experiments. Scale bars: 5 µm.

Journal of Cell Science (2017) 130, 2564-2578 doi:10.1242/jcs.197905

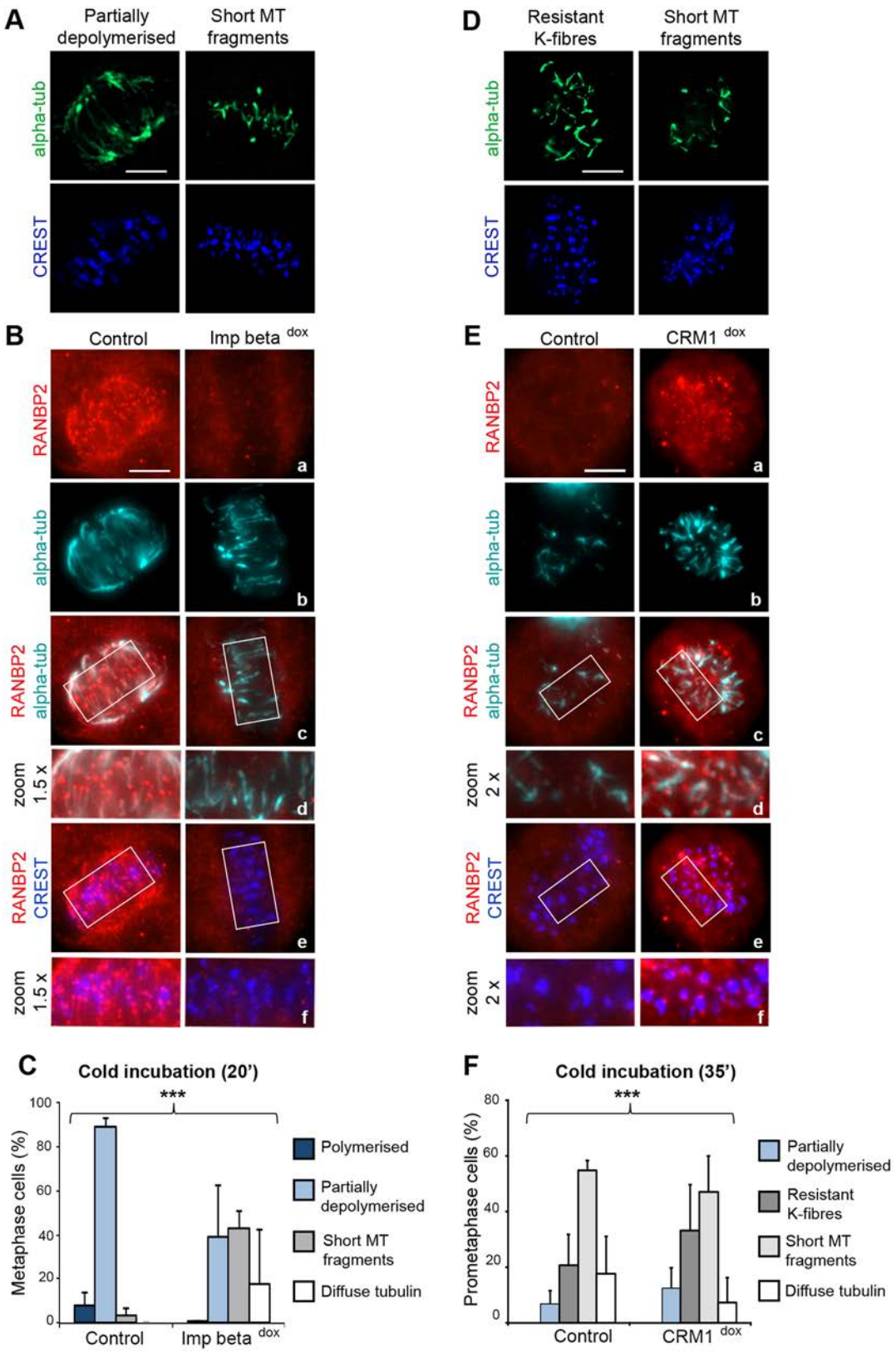

Fig. 7. CRM1 and importin-β affect MT stability. (A) Examples of MT depolymerisation phenotypes observed after 20 min incubation on ice. (B) Example MT patterns in control and importin-β-overexpressing cells (fewer cold-resistant MTs, concomitant with decreased RANBP2 localisation at metaphase KTs). (C) Histograms represent the frequency of MT phenotypes after cold incubation and show a significant shift towards severe MT depolymerisation phenotypes in importin-β versus control cultures (***P<0.0001, Fisher's exact test); n=240 cells per sample, five experiments. (D) Typical MT depolymerisation phenotypes after 35 min incubation on ice. (E) CRM1-overexpressing cells show more resistant K-fibres juxtaposed to RANBP2 at prometaphase KTs compared with controls. (F) Quantification of MT phenotypes in CRM1-induced, with predominant resistant K-fibres, versus control cultures (***P<0.0001, Fisher's exact test); n=220 cells per group, three experiments. Scale bars: 5 µm.

Journal of Cell Science (2017) 130, 2564-2578 doi:10.1242/jcs.197905

2013; Vecchione et al., 2016). In interphase transport, the interplay between RANBP2 and nuclear transport receptors is crucial for the correct distribution of protein cargos within cells. Here, we show that the spatiotemporal pattern of RANBP2 in mitosis depends on interactions with importin-β and CRM1, and impacts on relevant processes in mitotic progression.

The PLA approach developed here provides a valuable tool to investigate these interactions in space and time. We found that RANBP2 PLA products with either importin-β, or with CRM1, exhibit spatially and temporally regulated, mutually dependent patterns that have an inverse trend before and after chromosome biorientation. RANBP2–importin-β PLA products are abundant in prometaphase and localise at MTs, and then are downregulated from metaphase onwards. Conversely, RANBP2-CRM1 PLA signals increase in metaphase, when a fraction becomes visible at KTs, which remain KT-associated during segregation (Fig. 8). Our PLA studies also show that RANBP2 interactions trace the RRSU complex, because similar, parallel changes were observed when testing RANGAP1 instead of RANBP2 in PLA reactions. The variations detected in this study suggest an active role for importin-β in retaining the RRSU complex along MTs before chromosome biorientation, and for CRM1 in recruiting a fraction of the complex once KTs become bioriented.

How may these interactions form and vary during mitotic progression? In structural studies, importin-β interacts with RANBP2 via a NUP-binding domain in the N-terminal region, and FG-rich regions in RANBP2 (reviewed by Bednenko et al., 2003; Christie et al., 2016). CRM1 – together with RANGTP – interacts with RANGAP1 (Arnaoutov et al., 2005; Wu et al., 2013). CRM1 can also bind RANBP2 in a zinc-finger domain outside the importin-β-interacting FG-rich regions (Singh et al., 1999). Based on these data, the RANBP2-RANGAP1 complex can 'switch partners' via specific contacts with nuclear transport receptors: importin-β with RANBP2, CRM1 with RANGAP1 and possibly with a specific RANBP2 region. The switch does not disrupt the integrity within the RRSU complex itself. The 'preferred' RRSU partner in mitotic stages may simply reflect its physical proximity to transport vectors. Importin-β associates with mitotic MTs and poles via dynein (Ciciarello et al., 2004). CRM1 comprises fractions at centrosomes, MTs, and a fraction anchored to KTs via the NPC subcomplex NUP107-160 (Zuccolo et al., 2007). The RRSU may interact with one or the other transport receptor depending on its distance from them. Phosphorylation may further modulate local interactions. Indeed, importin-β interactions are influenced by the phosphorylation state of partners (Nardozzi et al., 2010). In addition, CDK1–cyclin-B1 activity is involved in mitotic phosphorylation of CRM1, and phosphorylated CRM1 shows higher affinity for RANGAP1 compared with non-phosphorylatable forms (Wu et al., 2013).

We also find that importin-β–RANBP2 PLA products form in cells lacking MTs, but their distribution is spread. Similarly, the lack of MT integrity did not affect RANBP2-CRM1 PLA formation, but prevented their localisation to KTs; thus MTs are an integral part of the RANBP2 'switch partners' model during mitosis.

We have generated HeLa cell lines to induce overexpression of either importin-β, or CRM1, in a controlled manner. High levels of

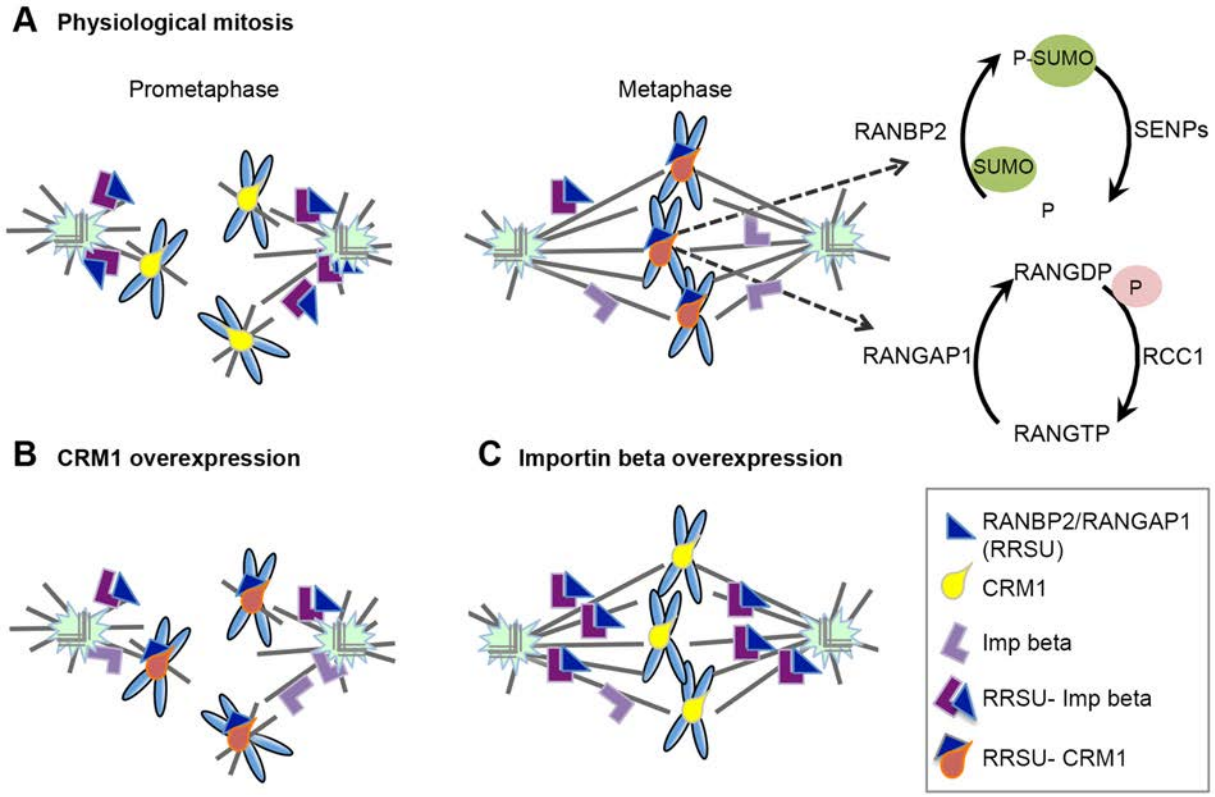

Fig. 8. Model for RANBP2-RANGAP1 recruitment to KTs. (A) Schematic representation of the spatial and temporal variations of RANBP2–SUMO-RANGAP1 (RRSU) interactions with transport factors during mitosis. In a physiological mitosis, RRSU recruitment to MT-attached KTs with CRM1 modulates local cycles of protein SUMOylation and of nucleotide turnover on RAN. (B) In CRM1-induced cells, RANBP2 recruitment at KTs is anticipated in prometaphase. (C) In importin-β-induced cells, RANBP2–importin-β PLA products are retained at MTs, while RANBP2-CRM1 decrease at KTs in metaphase. The altered timing (B), or impairment (C), of RANBP2 localisation at KTs affects in turn the accumulation of SUMO-TOP2A at centromeres and the stability of K-fibres.

Journal of Cell Science (2017) 130, 2564-2578 doi:10.1242/jcs.197905

overexpression of either receptor prevents mitotic entry altogether (Ciciarello et al., 2004; Roscioli et al., 2012), whereas mild overexpression of importin-β or CRM1, such as actually assessed in cancer samples (van der Watt et al., 2009), does not prevent mitosis and induces genetic instability during abnormal cell divisions. In our cell lines, induction of moderate importin-β overexpression retained RANBP2–importin-β PLA products along the spindle MTs and prevented their decrease in metaphase, unlike in physiological mitosis. Concomitant with this, the accumulation of CRM1-RANBP2 PLA products at metaphase KTs was impaired. Importantly, these cells failed to accumulate SUMO-TOP2A at centromeres, a feature that has been associated with the origin of aneuploidy. SUMO has been found to regulate both the centromere decatenation function of TOP2A (Dawlaty et al., 2008) and its interaction with haspin (Yoshida et al., 2016), which in turn acts in a regulatory cross-talk with the Aurora B kinase. The defective accumulation of SUMO-TOP2A at centromeres, associated with RANBP2 retention at MTs, might underlie at least some of the segregation defects recorded in importin-β-overexpression cells. Furthermore, associated with defective RANBP2 interaction with CRM1 at KTs, these cells also display decreased stability of mitotic MTs revealed by impaired K-fibre resistance to cold-induced depolymerisation.

Conversely, CRM1-overexpressing cells prematurely recruited RANBP2 to prometaphase KTs. That was associated with mis-segregation and generation of multinucleated cells. CRM1 overexpression therefore overrides the control mechanism that normally retains RANBP2–SUMO-RANGAP1 at prometaphase MTs and enables their delivery to KTs only after biorientation. This suggests that, under these conditions, RANBP2 is transferred to KTs at a stage at which MT attachments are not yet fully 'mature'. These attachments may be stabilised prematurely: indeed, cold assays revealed hyperstable K-fibres associated with precocious RANBP2 localisation at KTs. Interestingly, we observed in parallel the premature accumulation of SUMO-TOP2A at centromeres, which may cause deregulated sister chromatid decatenation before chromosomes are fully bioriented.

In conclusion, a model is beginning to emerge from the present data (Fig. 8), whereby the mitotic localisation of RANBP2–SUMO-RANGAP1 depends on the antagonistic actions of importin-β and CRM1. In turn, this affects functional features of centromeres and KTs. In this study, we have characterised SUMO-conjugated TOP2A and K-fibre stability as two paradigmatic targets of properly localised RANBP2 activity. It is reasonable to expect that other processes that depend on protein SUMOylation may be similarly altered under elevated levels of importin-β or CRM1.

Of note, several cancer types overexpress these karyopherins (Rensen et al., 2008; van der Watt et al., 2009) and inhibitors of nuclear transport processes are being developed with therapeutic purposes (Stelma et al., 2016; Mahipal and Malafa, 2016). The present data suggest that the relative abundance of importin-β and CRM1 is crucial to KT functions that depend on the RRSU complex.

MATERIALS AND METHODS

Cell culture, synchronisation and treatments

Human HeLa cells (American Tissue Culture Collection, CCL-2) were grown in DMEM supplemented with 10% fetal bovine serum, 2% L-glutamine, 2.5% HEPES and 2% penicillin-streptomycin at 37°C in 5% CO_2. Where indicated, cells were synchronised in 2 mM thymidine for 20–24 h to arrest the cell cycle at the G1-S transition, then released in medium containing 30 µM deoxycytidine. Cells were treated with 400 ng/ml NOC (Sigma-Aldrich) 10 h after thymidine release and harvested 4 h later. LMB (Enzo Life Sciences) was used at 20 nM in asynchronous cultures for 2 h.

Generation of stable cell lines for importin-β and CRM1

Inducible expression vectors for importin-β-EGFP and CRM1-EGFP were derived from the enhanced piggyBac (ePiggyBac) vector, carrying a tetracycline-responsive promoter element followed by a multicloning site. To generate epB-Bsd-TT-importin-β-EGFP, the sequence encoding importin-β–EGFP (Ciciarello et al., 2004) was PCR amplified using oligonucleotides pEGFP-N1_Fw_ClaI (GGCATCGATAGCGCTACCGG-ACTC) and pEGFP-N1_Rv (ACCTCTACAAATGTGGTATGGC). The PCR fragment was then digested and cloned between the ClaI and NotI sites in the epB-Bsd-TT plasmid, in which the puromycin resistance gene in the original epB-Puro-TT (Rosa et al., 2014) was replaced with a blasticidin resistance gene. The epB-Bsd-TT-CRM1-EGFP vector was generated by subcloning the CRM1-EGFP sequence (Roscioli et al., 2012) between the BamHI and NotI sites of epB-Bsd-TT. HeLa cells were co-trasfected with vector and hypb7 (encoding the transposase gene) using Lipofectamine (Invitrogen). Twenty-four hours after transfection, the medium was replaced with Tet-free DMEM supplemented with 3 µg/ml blasticidine-S hydrochloride (Sigma). Blasticidine-S-resistant foci were expanded and tested for expression after administration of 1 µg/ml doxycyline hyclate (dox, Santa Cruz Biotechnology).

RNA interference

RNA oligonucleotides were: RANBP2, 5′-GGACAGUGGGAUUGUAG-UGTT-3′ (Ambion); and GL2 (luciferase gene), 5′-CGUACGCGGAAU-ACUUCGATT-3′ (Ambion). For CRM1 a pool of three siRNAs was used (sc-35116, Santa Cruz Biotechnology). siRNA duplexes were diluted in serum-free OptiMem and transfected using Oligofectamine (Invitrogen), at 150 nM (RANBP2) and 20 nM (CRM1 and GL2) final concentrations.

Immunofluorescence

Cells grown on polylysine-coated coverslips were fixed using 3.7% paraformaldehyde in 30 mM sucrose, permeabilised in 0.1% Triton X-100 and incubated with antibodies. Primary antibodies are listed in Table S1. Secondary antibodies were conjugated to fluorescein isothiocyanate (FITC, green), Alexa 647 (far red), Cy3 (red) or 7-amino-4-methylcoumarin-3-acetic acid (AMCA, blue) (Jackson Immunoresearch Laboratories), or Texas Red (red, Vector Laboratories). DNA was stained with 0.1 µg/ml 4,6-diamidino-2-phenylindole (DAPI, Sigma-Aldrich). Coverslips were mounted in Vectashield (Vector Laboratories).

Proximity ligation assay (PLA)

The PLA method is based on recognition of the proteins of interest by primary antibodies, followed by secondary antibodies conjugated with oligonucleotide tails (called PLUS and MINUS). Connector oligonucleotides complementary to the secondary antibody-conjugated oligonucleotides are then added: when proteins are in close proximity (<30 nm), the connector oligonucleotides can pair with the PLUS and MINUS tails in a ligation step. This is followed by a rolling circle DNA amplification, visualised by a complementary fluorescent probe. Intramolecular PLA uses the same principle but uses primary antibodies directed against different regions of the same protein or against a protein and a candidate post-translational modification (here, TOP2A protein and SUMO-2/3 peptides). Duolink PLA kits were used following the Olink Bioscience protocol. Routinely, cells were blocked and incubated with primary antibody as for IF; anti-mouse MINUS and anti-rabbit PLUS PLA probes were then added and incubated in a pre-heated humidity chamber (60 min, 37°C). Subsequent hybridisation, ligation and detection steps were performed using the Duolink Detection kit according to the manufacturer's protocol. Primary antibodies are listed in Table S1.

MT depolymerisation assays

Uninduced (controls) or dox-induced (importin-β, CRM1) cultures were placed on ice for 20 or 35 min. At the end of incubation they were washed in

PTEMF buffer (20 mM Pipes, 10 mM EGTA, 1 mM $MgCl_2$) to preserve resistant MTs, fixed (3.7% PFA, 0.2% Triton X-100 in PTEMF), then processed for IF as described above.

Microscopy

Fixed samples were analysed under a Nikon Eclipse 90i microscope equipped with a Qicam Fast 1394 CCD camera (Qimaging). Single-cell images were taken using an immersion oil 100× objective (NA 1.3) and entire fields under a 40× objective (NA 0.75). Images were acquired using NIS-Elements AR 3.2 and 4.0 software (Nikon); three-dimensional deconvolution of 0.3–0.4 µm z-serial optical sections was performed using the 'AutoQuant' deconvolution module of NIS-Element AR 3.2/4.0. Creation of image projections was performed using the Maximum Intensity Projection (MIP, for quantitative analyses), and Extended Depth of Focus (EDF) functions of NIS-Element AR 3.2/4.0. IF signals were quantitatively analysed using NIS-Element AR 3.2/4.0 (nd2 file format); external background correction was applied and the sum intensity of signals on indicated selected areas was measured. PLA spots were counted on images acquired in three dimensions. In the manual count mode, PLA spots were counted in each individual plane. In the automatic mode, images were processed using the MIP method (therefore losing quantitative information for separate planes), activating the 'spot detection' and 'count objects' tools of NIS-Element AR 3.2/4.0. All figures shown in this work represent MIP images unless specified otherwise. Images were processed with Adobe Photoshop CS 8.0.

Time-lapse imaging

Cells were seeded in µ-Slide (chambered coverslip) with 4 or 8 wells (80426/80821, IbiTreat; Ibidi) in Phenol Red-free DMEM supplemented as above. During recording, cell cultures were kept at 37°C in a temperature- and CO_2-controlled microscope stage incubator (Okolab). Cultures were recorded under an automated inverted microscope (Ti Eclipse; Nikon) equipped with a DS-Qi1MC camera, an Intensilight C-HGFIE lamp, and NIS-Elements 3.1 software (all from Nikon). Phase-contrast (60×, 0.7 NA) objective was used. Cells were recorded for 6–24 h; phase-contrast images were taken every 15 min and GFP fluorescence images every 60 min.

Western immunoblotting

HeLa cells were lysed in RIPA buffer (50 mM Tris-HCl, pH 8, 150 mM NaCl, 1% NP40, 1 mM EGTA, 1 mM EDTA, 0.1% SDS, 0.25% sodium deoxycholate) supplemented with protease (05892791001, Roche) and phosphatase (PhoSTOP, 04906837001, Roche) inhibitors. Proteins (40 µg per lane) were separated through SDS-PAGE and transferred to nitrocellulose filters (Protran BA83, Whatman) in a semi-dry system (Bio-Rad). Blocking and antibody incubations were in TBS (10 mM Tris-HCl, pH 7.4, 150 mM NaCl) containing 0.1% Tween 20 and 5% low-fat milk. Primary and secondary antibodies were incubated for 1 h at room temperature. Primary antibodies are listed in Table S1. HRP-conjugated secondary antibodies (Santa Cruz Biotechnology) were revealed using the ECL detection system (GE Healthcare) on Hyperfilm-ECL films (GE Healthcare).

Acknowledgements

We are grateful to Paola Rovella for experimental contributions to this work.

Competing interests

The authors declare no competing or financial interests.

Author contributions

Conceptualization: A.R., P.L.; Methodology: E.G., V.d.T., M.D., A.V., S.M., R.D.S., A.R., P.L.; Validation: E.G., V.d.T., M.D., A.V., S.M., R.D.S., A.R., P.L.; Formal analysis: E.G., V.d.T., M.D., A.V., S.M., P.L.; Investigation: E.G., V.d.T., M.D., A.V., S.M., R.D.S.; Resources: A.R.; Data curation: E.G., V.d.T., M.D., A.V., P.L.; Writing – original draft: P.L.; Writing – review and editing: E.G., V.d.T., A.V., A.R.; Supervision: P.L.; Funding acquisition: P.L.

Funding

This work was supported by Associazione Italiana per la Ricerca sul Cancro (AIRC-IG14534) and Consiglio Nazionale delle Ricerche InterOmics Flagship Projects (grants IBISA and SYNLETHER).

Supplementary information

Supplementary information available online at
http://jcs.biologists.org/lookup/doi/10.1242/jcs.197905.supplemental

References

Arnaoutov, A., Azuma, Y., Ribbeck, K., Joseph, J., Boyarchuk, Y., Karpova, T., McNally, J. and Dasso, M. (2005). Crm1 is a mitotic effector of Ran-GTP in somatic cells. *Nat. Cell Biol.* **7**, 626-632.

Azuma, Y., Arnaoutov, A. and Dasso, M. (2003). SUMO-2/3 regulates topoisomerase II in mitosis. *J. Cell Biol.* **163**, 477-487.

Bednenko, J., Cingolani, G. and Gerace, L. (2003). Nucleocytoplasmic transport: navigating the channel. *Traffic* **4**, 127-135.

Budhu, A. S. and Wang, X. W. (2005). Loading and unloading: orchestrating centrosome duplication and spindle assembly by Ran/Crm1. *Cell Cycle* **4**, 1510-1514.

Cavazza, T. and Vernos, I. (2015). The Ran GTPase pathway: from nucleo-cytoplasmic transport to spindle assembly and beyond. *Front. Cell Dev. Biol.* **3**, 82.

Cha, K., Sen, P., Raghunayakula, S. and Zhang, X. D. (2015). The cellular distribution of RanGAP1 is regulated by CRM1-mediated nuclear export in mammalian cells. *PLoS ONE* **10**, e0141309.

Chen, T., Sun, Y., Ji, P., Kopetz, S. and Zhang, W. (2015). Topoisomerase IIα in chromosome instability and personalized cancer therapy. *Oncogene* **34**, 4019-4031.

Christie, M., Chang, C.-W., Róna, G., Smith, K. M., Stewart, A. G., Takeda, A. A. S., Fontes, M. R. M., Stewart, M., Vértessy, B. G., Forwood, J. K. et al. (2016). Structural biology and regulation of protein import into the nucleus. *J. Mol. Biol.* **428**, 2060-2090.

Ciciarello, M., Mangiacasale, R., Thibier, C., Guarguaglini, G., Marchetti, E., Di Fiore, B. and Lavia, P. (2004). Importin β is transported to spindle poles during mitosis and regulates Ran-dependent spindle assembly factors in mammalian cells. *J. Cell Sci.* **117**, 6511-6522.

Ciciarello, M., Mangiacasale, R. and Lavia, P. (2007). Spatial control of mitosis by the GTPase Ran. *Cell. Mol. Life Sci.* **64**, 1891-1914.

Clarke, P. R. and Zhang, C. (2008). Spatial and temporal coordination of mitosis by Ran GTPase. *Nat. Rev. Mol. Cell Biol.* **9**, 464-477.

Cubeñas-Potts, C., Goeres, J. D. and Matunis, M. J. (2013). SENP1 and SENP2 affect spatial and temporal control of sumoylation in mitosis. *Mol. Biol. Cell* **24**, 3483-3495.

Cubeñas-Potts, C., Srikumar, T., Lee, C., Osula, O., Subramonian, D., Zhang, X.-D., Cotter, R. J., Raught, B. and Matunis, M. J. (2015). Identification of SUMO-2/3 modified proteins associated with mitotic chromosomes. *Proteomics* **15**, 763-772.

Dasso, M. (2006). Ran at kinetochores. *Biochem. Soc. Trans.* **34**, 711-715.

Dawlaty, M. M., Malureanu, L., Jeganathan, K. B., Kao, E., Sustmann, C., Tahk, S., Shuai, K., Grosschedl, R. and van Deursen, J. M. (2008). Resolution of sister centromeres requires RanBP2-mediated SUMOylation of topoisomerase IIalpha. *Cell* **133**, 103-115.

Eifler, K. and Vertegaal, A. C. (2015). SUMOylation-mediated regulation of cell cycle progression and cancer. *Trends Biochem. Sci.* **40**, 779-793.

Flotho, A. and Werner, A. (2012). The RanBP2/RanGAP1*SUMO1/Ubc9 complex: a multisubunit E3 ligase at the intersection of sumoylation and the Ran GTPase cycle. *Nucleus* **3**, 429-432.

Forbes, D. J., Travesa, A., Nord, M. S. and Bernis, C. (2015). Nuclear transport factors: global regulation of mitosis. *Curr. Opin. Cell Biol.* **35**, 78-90.

Forgues, M., Difilippantonio, M. J., Linke, S. P., Ried, T., Nagashima, K., Feden, J., Valerie, K., Fukasawa, K. and Wang, X. W. (2003). Involvement of Crm1 in hepatitis B virus X protein-induced aberrant centriole replication and abnormal mitotic spindles. *Mol. Cell. Biol.* **23**, 5282-5292.

Hashizume, C., Kobayashi, A. and Wong, R. W. (2013). Down-modulation of nucleoporin RanBP2/Nup358 impaired chromosomal alignment and induced mitotic catastrophe. *Cell Death Dis.* **4**, e854.

Joseph, J., Tan, S.-H., Karpova, T. S., McNally, J. G. and Dasso, M. (2002). SUMO-1 targets RanGAP1 to kinetochores and mitotic spindles. *J. Cell Biol.* **156**, 595-602.

Joseph, J., Liu, S.-T., Jablonski, S. A., Yen, T. J. and Dasso, M. (2004). The RanGAP1-RanBP2 complex is essential for microtubule-kinetochore interactions in vivo. *Curr. Biol.* **14**, 611-617.

Kalab, P. and Heald, R. (2008). The RanGTP gradient – a GPS for the mitotic spindle. *J. Cell Sci.* **121**, 1577-1586.

Kaláb, P., Pralle, A., Isacoff, E. Y., Heald, R. and Weis, K. (2006). Analysis of a RanGTP-regulated gradient in mitotic somatic cells. *Nature* **440**, 697-701.

Mahajan, R., Delphin, C., Guan, T., Gerace, L. and Melchior, F. (1997). A small ubiquitin-related polypeptide involved in targeting RanGAP1 to nuclear pore complex protein RanBP2. *Cell* **88**, 97-107.

Mahipal, A. and Malafa, M. (2016). Importins and exportins as therapeutic targets in cancer. *Pharmacol. Ther.* **164**, 135-143.

Matunis, M. J., Coutavas, E. and Blobel, G. (1996). A novel ubiquitin-like modification modulates the partitioning of the Ran-GTPase-activating protein RanGAP1 between the cytosol and the nuclear pore complex. *J. Cell Biol.* **135**, 1457-1470.

Matunis, M. J., Wu, J. and Blobel, G. (1998). SUMO-1 modification and its role in targeting the Ran GTPase-activating protein, RanGAP1, to the nuclear pore complex. *J. Cell Biol.* **140**, 499-509.
Mukhopadhyay, D. and Dasso, M. (2010). The fate of metaphase kinetochores is weighed in the balance of SUMOylation during S phase. *Cell Cycle* **15**, 3194-3201.
Nachury, M. V., Maresca, T. J., Salmon, W. C., Waterman-Storer, C. M., Heald, R. and Weis, K. (2001). Importin beta is a mitotic target of the small GTPase Ran in spindle assembly. *Cell* **104**, 95-106.
Nardozzi, J. D., Lott, K. and Cingolani, G. (2010). Phosphorylation meets nuclear import: a review. *Cell Commun. Signal.* **8**, 32.
Pichler, A., Gast, A., Seeler, J. S., Dejean, A. and Melchior, F. (2002). The nucleoporin RanBP2 has SUMO1 E3 ligase activity. *Cell* **108**, 109-120.
Prosser, S. L. and Pelletier, L. (2017). Mitotic spindle assembly in animal cells: a fine balancing act. *Nat. Rev. Mol. Cell Biol.* **18**, 187-201.
Rensen, W. M., Mangiacasale, R., Ciciarello, M. and Lavia, P. (2008). The GTPase Ran: regulation of cell life and potential roles in cell transformation. *Front. Biosci.* **13**, 4097-4121.
Ritterhoff, T., Das, H., Hofhaus, G., Schröder, R. R., Flotho, A. and Melchior, F. (2016). The RanBP2/RanGAP1*SUMO1/Ubc9 SUMO E3 ligase is a disassembly machine for Crm1-dependent nuclear export complexes. *Nat. Commun.* **7**, 11482.
Rosa, A., Papaioannou, M. D., Krzyspiak, J. E. and Brivanlou, A. H. (2014). miR-373 is regulated by TGFβ signaling and promotes mesendoderm differentiation in human embryonic stem cells. *Dev. Biol.* **391**, 81-88.
Roscioli, E., Di Francesco, L., Bolognesi, A., Giubettini, M., Orlando, S., Harel, A., Schininà, M. E. and Lavia, P. (2012). Importin beta negatively regulates multiple aspects of mitosis including RANGAP1 recruitment to kinetochores. *J. Cell Biol.* **196**, 435-450.
Ryu, H., Furuta, M., Kirkpatrick, D., Gygi, S. P. and Azuma, Y. (2010). PIASy-dependent SUMOylation regulates DNA topoisomerase IIalpha activity. *J. Cell Biol.* **191**, 783-794.
Salina, D., Enarson, P., Rattner, J. B. and Burke, B. (2003). Nup358 integrates nuclear envelope breakdown with kinetochore assembly. *J. Cell Biol.* **162**, 991-1001.
Singh, B. B., Patel, H. H., Roepman, R., Schick, D. and Ferreira, P. A. (1999). The zinc finger cluster domain of RanBP2 is a specific docking site for the nuclear export factor, exportin-1. *J. Biol. Chem.* **274**, 37370-37378.
Stelma, T., Chi, A., van der Watt, P. J., Verrico, A., Lavia, P. and Leaner, V. D. (2016). Targeting nuclear transporters in cancer: diagnostic, prognostic and therapeutic potential. *IUBMB Life.* **68**, 268-280.
Swaminathan, S., Kiendl, F., Körner, R., Lupetti, R., Hengst, L. and Melchior, F. (2004). RanGAP1*SUMO1 is phosphorylated at the onset of mitosis and remains associated with RanBP2 upon NPC disassembly. *J. Cell Biol.* **164**, 965-971.
Torosantucci, L., De Luca, M., Guarguaglini, G., Lavia, P. and Degrassi, F. (2008). Localized RanGTP accumulation promotes microtubule nucleation at kinetochores in somatic mammalian cells. *Mol. Biol. Cell* **19**, 1873-1882.
Tulu, U. S., Fagerstrom, C., Ferenz, N. P. and Wadsworth, P. (2006). Molecular requirements for kinetochore-associated microtubule formation in mammalian cells. *Curr. Biol.* **16**, 536-541.
van der Watt, P. J., Maske, C. P., Hendricks, D. T., Parker, M. I., Denny, L., Govender, D., Birrer, M. J. and Leaner, V. D. (2009). The Karyopherin proteins, Crm1 and Karyopherin beta1, are overexpressed in cervical cancer and are critical for cancer cell survival and proliferation. *Int. J. Cancer* **124**, 1829-1840.
Vecchione, L., Gambino, V., Raaijmakers, J., Schlicker, A., Fumagalli, A., Russo, M., Villanueva, A., Beerling, E., Bartolini, A., Mollevi, D. G. et al. (2016). A vulnerability of a subset of colon cancers with potential clinical utility. *Cell* **165**, 317-330.
Vuoriluoto, M., Laine, L. J., Saviranta, P., Pouwels, J. and Kallio, M. J. (2011). Spatio-temporal composition of the mitotic chromosomal passenger complex detected using in situ proximity ligation assay. *Mol. Oncol.* **5**, 105-111.
Wan, J., Subramonian, D. and Zhang, X.-D. (2012). SUMOylation in control of accurate chromosome segregation during mitosis. *Curr. Protein Pept. Sci.* **13**, 467-481.
Werner, A., Flotho, A. and Melchior, F. (2012). The RANBP2/RanGAP1*SUMO1/Ubc9 complex is a multisubunit SUMO E3 ligase. *Mol. Cell* **46**, 287-298.
Wu, J., Matunis, M. J., Kraemer, D., Blobel, G. and Coutavas, E. (1995). Nup358, a cytoplasmically exposed nucleoporin with peptide repeats, Ran-GTP binding sites, zinc fingers, a cyclophilin A homologous domain, and a leucine-rich region. *J. Biol. Chem.* **270**, 14209-14213.
Wu, Z., Jiang, Q., Clarke, P. R. and Zhang, C. (2013). Phosphorylation of Crm1 by CDK1-cyclin-B promotes Ran-dependent mitotic spindle assembly. *J. Cell Sci.* **126**, 3417-3428.
Yokoyama, N., Hayashi, N., Seki, T., Panté, N., Ohba, T., Nishii, K., Kuma, K., Hayashida, T., Miyata, T., Aebi, U. et al. (1995). A giant nucleopore protein that binds Ran/TC4. *Nature* **376**, 184-188.
Yoshida, M. M., Ting, L., Gygi, S. P. and Azuma, Y. (2016). SUMOylation of DNA topoisomerase IIα regulates histone H3 kinase Haspin and H3 phosphorylation in mitosis. *J. Cell Biol.* **213**, 665-678.
Zhang, X.-D., Goeres, J., Zhang, H., Yen, T. J., Porter, A. C. G. and Matunis, M. J. (2008). SUMO-2/3 modification and binding regulate the association of CENPE with kinetochores and progression through mitosis. *Mol. Cell* **29**, 729-741.
Zuccolo, M., Alves, A., Galy, V., Bolhy, S., Formstecher, E., Racine, V., Sibarita, J. B., Fukagawa, T., Shiekhattar, R., Yen, T. et al. (2007). The human Nup107-160 nuclear pore subcomplex contributes to proper kinetochore functions. *EMBO J.* **26**, 1853-1864.